Collective effects for long bunches in dual harmonic RF systems*

AN Shi-Zhong(安世忠)[1;1)] Klaus Bongardt[2] Rudolf Maier[2]
TANG Jing-Yu(唐靖宇)[3] ZHANG Tian-Jue(张天爵)[1]

1 (China Institute of Atomic Energy, Beijing 102413, China)
2 (IKP, FZ Juelich, 52425 Juelich, Germany)
3 (Institute of High Energy Physics, CAS, Beijing 100049, China)

Abstract The storage of long bunches for large time intervals needs flattened stationary buckets with a large bucket height. Collective effects from the space charge and resistive impedance are studied by looking at the incoherent particle motion for the matched and mismatched bunches. Increasing the RF amplitude with particle number provides r.m.s wise matching for modest intensities. The incoherent motion of large amplitude particles depends on the details of the RF system. The resulting debunching process is a combination of the too small full RF acceptance together with the mismatch, enhanced by the collective effects. Irregular single particle motion is not associated with the coherent dipole instability. For the stationary phase space distribution of the Hofmann-Pedersen approach and for the dual harmonic RF system, stability limits are presented, which are too low if using realistic input distributions. For single and dual harmonic RF system with d=0.31, the tracking results are shown for intensities, by a factor of 3 above the threshold values. Small resistive impedances lead to coherent oscillations around the equilibrium phase value, as energy loss by resistive impedance is compensated by the energy gain of the RF system.

Key words resistive impedance, incoherent motion, halo formation, coherent dipole instability

PACS 29.27.Ac

1 Introduction

In the previous paper[1], properties of the dual harmonic RF systems are discussed for emittance-dominated long bunches below transition. Long bunches can be r.m.s wise matched either in single or in dual harmonic system with d=0.31. But even for shorter bunches with 20% larger energy spread and zero intensity, the bucket height is too small for the single harmonic system. Findings are valid in general, only depending on the new voltage factor $R(N)$ to preserve the r.m.s bunch length and on the synchrotron oscillation period. $R(N)$=2 is the boundary between the emittance and the space charge (SC)-dominated bunches. Even for the modest intensities, $R(N)$=2, not increasing the RF voltage leads to debunching for the single harmonic RF system[1].

Adding low frequency resistive impedances modifies physics, analyzed by the motion of test particles and realistic, but different input distributions. Emittance dilution and debunching are evaluated with the 1D ORBIT[2] tracking code for the 1 GeV cooled bunches in the HESR synchrotron, part of the GSI FAIR project[3]. Debunching of large amplitude particles is a combination of the too small full RF acceptance with the mismatch, enhanced by the collective effects. Equilibrium phase values are obtained even for the SC-dominated bunches with high intensity, suffering from emittance dilution, but not from coherent dipole instability.

All results are valid for staying below transition.

2 Energy change by resistive impedances

Energy change of a test particle within a vacuum chamber, traveling behind a bunch, is described either by time dependent wake fields or by frequency dependent longitudinal impedances, connected by Fourier transformation. For a single bunch, retarding voltage

Received 26 October 2006, Revised 3 September 2007
* Supported by National Natural Science Foundation of China (10075065)
1) E-mail: szan@ciae.ac.cn

$V_{\rm r}(\phi)$ in time domain[4, 5] is given by a continuous Fourier transformation:

$$V_{\rm r}(\phi) = -\frac{1}{2\pi}\int_{-\infty}^{\infty}(\mathrm{Im}Z_{//}(\omega)\sin(\omega\phi)+ \mathrm{Re}Z_{//}(\omega)\cos(\omega\phi))I(\omega)\mathrm{d}\omega\,, \quad (1)$$

where $Z_{//}(\omega)$ is the complex longitudinal impedance and $I(\omega)$ is the Fourier component of current distribution $I(\phi)$. Impedances have symmetry property: $Z_{//}(-\omega)=Z_{//}(\omega)$.

Single bunch with symmetric line density $\lambda(\phi)$ in circular ring with the circumference $C=2\pi R$ leads to the retarding voltage $V_{\rm r}(\phi)$, given by discrete Fourier transformation:

$$V_{\rm r}(\phi) = -(Nq\beta c)/R\sum\big(\lambda_n[\sin(n\phi)\mathrm{Im}Z(n)+ \cos(n\phi)\mathrm{Re}Z(n)]\big), \quad n\geqslant 1, \quad (2)$$

voltage $V_{\rm r}(\phi)$ replaces $V_{\rm SC}(\phi)$ in single particle Eq. (3) of Ref. [1]. Symmetric line densities $\lambda(\phi)$ and imaginary impedances mean asymmetric retarding voltages $V_{\rm r}(\phi)$, and no net energy loss of the bunch. Resistive impedances instead mean the symmetric retarding voltages $V_{\rm r}(\phi)$, and therefore the net energy loss of the bunch. For $Z_{//}(n)=$ constant up to high frequencies, the energy change curve is identical with the line density $\lambda(\phi)$.

Emittance dilution is caused in all cases except for a parabolic line density and pure SC impedance, $Z_{//}^{\rm SC}/n=$ constant beyond high frequency cut-off[4, 5], leading to exact linear retarding voltage.

Figure 1 shows the energy change of test particles after 10^3 turns for either the parabolic or the Gaussian line density, obtained from 1D tracking with ORBIT, caused by low frequency normalized resistive impedance $Z_{//}/n=50\ \Omega$ for n=1, 4. The generalized resistive impedances used, dominated by the RF system, are not the complex thick wall impedances, where both parts scale like $1/\sqrt{n}$ for high frequencies[4, 5].

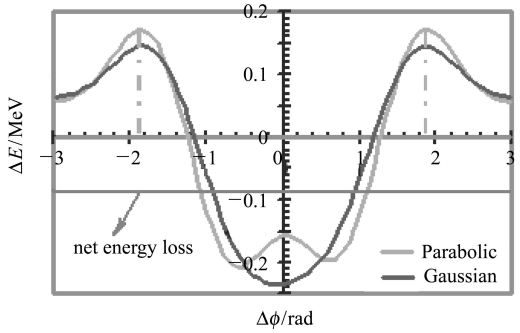

Fig. 1. Energy change of individual particles (The dashed lines are the boundaries of parabolic density).

Assumed is 1 GeV bunch with 10^{13} particles in the HESR ring, see Table 1. Both bunches have identical r.m.s phase value of 0.78 rad, but the parabolic line density is limited in phase to $\sqrt{5}\times$ r.m.s value. The maximal energy loss occurs for particles at the bunch center, whereas the energy gain is maximal at the bunch edges. Indicated is also the net energy loss after 10^3 turns of -0.09 MeV, almost identical for both cases. Local minimum at the bunch center for the parabolic density is due to the large r.m.s phase value and $Z_{//}/n=$ constant at low frequencies. Energy gains of particles near the bucket end are also evaluated using the test particles. 500 Ω SC impedance of HESR[3], much larger than the contribution from all technical components, shifts the maximal energy loss towards positive value.

The main parameters of the HESR synchrotron, staying below transition, are given in Table 1.

Table 1. The main HESR parameters.

circumference, $\gamma_{\rm t}$	574 m, 6.5 i
energy range	0.83—14.1 GeV
stochastic cooling	3—14.1 GeV
electron cooling	0.83—8 GeV
high luminosity mode:	full energy range,
$\sigma_{\rm p}/p\sim 10^{-4}$	up to 10^{11} particles
high resolution mode:	up to 8 GeV,
$\sigma_{\rm p}/p\sim 4\times 10^{-5}$	10^{10} particles
curved cold dipole	48 magnets, <3.6 T

Assuming 6-fold symmetry in arcs[3], but discussed is also 4-fold symmetry with only 32 dipoles. The electron and stochastic cooling equipment allows the adjustment of r.m.s momentum spread $\sigma_{\rm p}/p$ for the internal target experiments. Single bunches up to 10^{11} particles are injected at 3 GeV. Each 180° arc uses 24 cold dipoles. Two dispersion free straight sections, each 130 m in length, provide space for the electron cooler and experiments. The cold sections have a total length of 500 m, and the warm sections of 74 m. A 10% time gap improves the lifetime of anti-protons.

3 Collective effects for $R(N)=2$

3.1 Coherent dipole oscillations

The 1D tracking results from ORBIT are shown in Fig. 2 for 1 GeV bunch in the HESR ring. A Gaussian bunch is used, N=10^{13}, with 400 m in length or the bunching factor B=0.7, the r.m.s phase value 0.78 rad, the r.m.s energy spread $\sigma_{\rm E}$ of 0.6 MeV resp. 4×10^{-4} r.m.s momentum spread. The matched voltages for the first and second harmonics are: 2.3 kV× (1,−0.31) resp. 1.7 kV×(1,0) for dual (d=0.31) resp. single harmonic (d=0) RF systems, twice the values for zero intensity, which means $R(N)$=2, indepen-

dent of distribution. 5000 macro particles and 64 frequency bins are used.

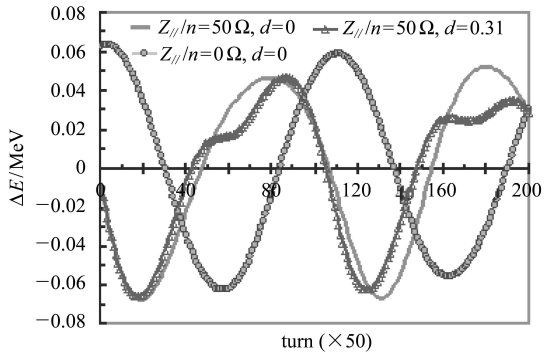

Fig. 2. The dipole oscillations for $R(N)$=2, with & without $Z_{//}/n$=50 Ω for n=1,4.

The resulting dipole oscillations are shown for long bunches in either the dual harmonic (d=0.31) or the single harmonic (d=0) RF system, without and with low frequency resistive impedances. Without resistive impedances, the dipole oscillations for $R(N)$=2 are almost identical and undamped for both RF systems, as SC forces lead to similar tune spread, but it is different from the zero intensity case[6]. Here we have the damped oscillation with decoherence time of only 1.5×10^4 turns for the single harmonic, but 7.2×10^4 turns for the dual harmonic[1]. Dipole oscillations are excited by the initial energy shift of 0.06 MeV.

Adding low frequency resistive components first causes energy loss, followed by dipole oscillations with more than one frequency for the dual harmonic system. The maximal energy loss of −0.07 MeV occurs after 10^3 turns, which is 3 times smaller than the greatest single particle energy loss, as shown in Fig. 1. The maximal phase displacement due to resistive impedance is about 0.12 rad, but oscillates around the equilibrium phase value, see Fig. 7. For long bunches, high frequency resistive impedances do not cause net energy loss.

Dipole oscillations are independent of the details of the input distribution, but depend on the chosen RF system. For small mismatch and initial shift of bunch center quadrupole resp. dipole mode frequencies $\omega_{\rm Q}(N)$ resp. $\omega_{\rm D}(N)$ are connected by[1, 7]:

$$\omega_{\rm Q}^2(N)/\omega_{\rm D}^2(N)=(1+3R(N))/R(N)\,. \qquad (3)$$

After subtracting the dipole oscillations, the coherent quadrupole oscillations are only weakly effected by the resistive impedances.

1D ORBIT calculations ignore the radial-axial coupling, as the SC impedance only depends on the b/a ratio, where the pipe radius b and the beam radius a are the averaged values. As the synchrotron period is much longer than the transverse one, excitation of radial-axial modes in circular rings is not very likely. However for high intensity linacs, where all 3 radii are similar, the mode coupling cannot be ignored[1].

3.2 Motion of large amplitude particles, d=0

The coherent first and second order moments, with SC and resistive impedance, are quite similar for the dual or single harmonic systems. But the incoherent single particle motion is suffering from debunching for d=0, as RF acceptance is too small[1].

In Fig. 3, the incoherent single particle trajectories are shown every 100 turns, in total 2×10^4 turns, in the single harmonic RF system for shorter bunch, either the Gaussian or the elliptical phase space distribution, but with 20% increased energy spread[1]. An elliptical distribution, leading to parabolic line density has less tails than a Gaussian one, as limited to $\sqrt{5}\times$ r.m.s phase resp. energy values. For the same r.m.s values, the collective effects are more dominant for shorter bunches, as reduced synchrotron tune spread. Also shown is the full RF acceptance, leading to the bucket height of only 2.5 MeV. All three single particle trajectories start at −2 MeV and zero phases, the maximal energy spread of all mismatched bunches, as elliptical distributions are shifted by −0.4 MeV.

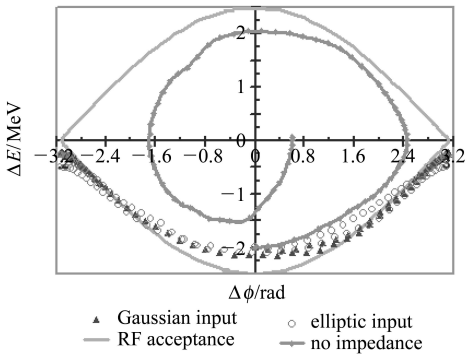

Fig. 3. The movement of test particles, initially at −2 MeV, with or without resistive impedance.

Without resistive impedances, a test particle performs the damped synchrotron oscillations but with more than one frequency, as the coherent dipole and quadrupole oscillations are present. The energy axis is crossed after 4×10^3 turns. About 5/4 synchrotron oscillations are performed after 2×10^4 turns. But adding resistive impedances $Z_{//}/n$=50 Ω for n=1,4, debunching of test particles occurs for both cases. An equivalent of 5/4 synchrotron oscillations is performed after 2×10^4 turns.

3.3 Debunching due to resistive impedances

Single particles with (−2 MeV, 0 rad) are inside the full RF acceptance, but with loose energy due to the mismatch[1] and resistive impedances. After about 2×10^3 turns, the energy loss due to resistive impedances is visible, as the test particles are now in front of the bunch center. 90° phase rotation is reached after 4×10^3 turns, both test particles have 0.25 MeV energy loss as predicted by Fig. 1, which are outside the full RF acceptance and have reached the bucket boundary. Particles belong to different RF buckets now, assuming to be identical. Therefore the phase value is changed from positive to negative value.

Synchrotron motion brings the particle back to the dense core and therefore it is inside the full RF acceptance again, as SC weakens the external voltage and the particles gain energy due to the resistive impedances, as they are behind the bunch center. After 1×10^4 turns, both test particles are again at small phase values. After the next 90° phase rotation, the test particles have reached the bucket boundary, but with increased energy loss of −0.5 MeV and their phase value is again changed from positive to negative value. After 2×10^4 turns, both test particles are back at small energy values, the elliptical one is somewhat behind the Gaussian one.

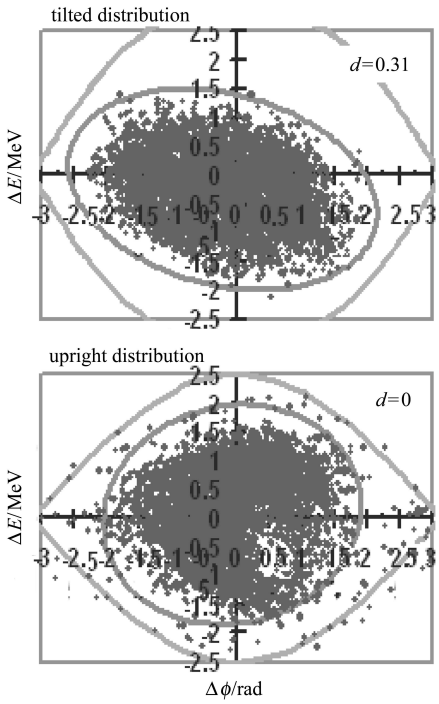

Fig. 4. Distributions after 2×10^4 turns with the elliptical boundary and full RF acceptance.

The full RF acceptance is not the exact boundary with SC forces, but quantifies the amount of debunching. Resulting filamented phase space distribution for the whole bunch is shown in Fig. 4.

By using a resistive impedance of $Z_{//}/n$=50 Ω only for n=1, from 6×10^3 turns on particles have always positive energy spread, suffering from the debunching process. The change of energy is given by 0.04 MeV $\cos\phi$, resulting in net energy loss of −0.02 MeV, compared with −0.09 MeV in Fig. 1.

The irregular motion of large amplitude particles is a combination of the too small full RF acceptance with the mismatch, enhanced by the collective effects.

Strong SC or more particles lead to larger full RF acceptance $\sim\sqrt{R(N)}$. The maximal energy loss increases less than linear with the particle number N, as coherent oscillation frequencies are increased $\sim\sqrt{R(N)}$. The resulting large dipole amplitude shifts the whole distribution towards the stable fix points. The innermost particles gain much more energy due to the mismatch[1]. As a consequence, particles with large amplitude can leave their RF bucket in spite of the increased bucket height. Simulation result is shown below for a SC-dominated bunch with $R(N)=4$, where distribution is changing.

4 Emittance & SC-dominated bunches

4.1 Emittance-dominated bunches, $R(N)=2$

The resulting phase space distributions after 2×10^4 turns are shown in Fig. 4 for injecting shorter elliptical bunches, 20% increased energy spread, in either dual or single harmonic system. Bunch is shifted by −0.4 MeV initially, 10^{13} particles and resistive impedances of $Z_{//}/n$=50 Ω for n=1,4 are used.

For the dual harmonic system, the obtained phase space distribution is quite similar to the results for the mismatched Gaussian one without initial shift and resistive impedances[1], as large bucket height of 3 MeV. The maximal incoherent energy loss of 0.25 MeV, see Fig. 1, does not lead to debunching. Particles are near the elliptical phase space boundary of 8× initial r.m.s emittance, well inside the RF acceptance.

For single harmonic instead, where the bucket height is only 2.5 MeV, large amplitude particles suffer from debunching, see Fig. 3. The r.m.s emittance is increased by 33% and the obtained phase space distribution is filamented. 4% of the particles are outside the elliptical phase space boundary of 8× initial r.m.s emittance. Only 0.4% of the particles have phase values above ±2.5 rad, but 0.6% of the particles are outside the full RF acceptance.

Using the mismatched Gaussian distribution as input leads to similar results after 2×10^4 turns for the

dual and single RF systems, as expected from Fig. 3. Neglecting the resistive impedance substantially reduces the debunching and halo formation[1].

4.2 SC-dominated bunch, $R(N)=4, d=0$

Increasing the particle number by a factor of 3 leads to $R(N)$=4 and bucket height of 3.5 MeV. The resulting phase space distribution after 2×10^4 turns is shown in Fig. 5 for injecting the matched elliptical bunch, and for having no resistive impedance and no initial shift.

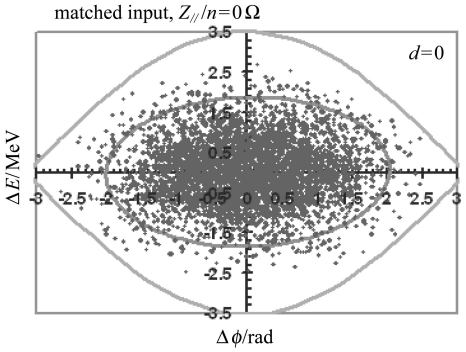

Fig. 5. Distribution after 2×10^4 turns with elliptical boundary and full RF acceptance.

After 2×10^4 turns, the r.m.s emitance is increased by 40% and about 15% of the particles of an elliptical phase space boundary of 8× initial r.m.s emittance. But all particles stay inside the full RF acceptance. Much less filamentation occurs for d=0.31 due to the enlarged full RF acceptance with 4.24 MeV bucket height.

Shorter bunch with 20% larger energy spread together with $Z_{//}/n$=50 Ω for n=1,4 leads to the similar filamented distribution, as shown in Fig. 4, but much more halo formation and particles near the stable fix points. After 2×10^4 turns, the r.m.s emittance is increased by 50%, about 20% of the particles are outside the elliptical phase space boundary of 8× initial r.m.s emittance. About 2% of the particles have phase values above ±2.5 rad. But only 0.2% of the particles are suffering from the debunching process, as the enlarged full RF acceptance.

The resistive impedances shift distribution by the maximal phase value of 0.3 rad, reached after 2×10^3 turns, followed by oscillation around the equilibrium phase value, see Fig. 7.

Using different energies or other lattice parameters, and in addition, choosing other SC and resistive impedances, will change the synchrotron period and the details of the debunching process, but not the underlying physics. Only low frequency components are relevant for long bunches.

Debunching of large amplitude particles is a combination of the too small full RF acceptance with the mismatch, enhanced by the collective effects. Mismatch is not possible for self-consistent phase space distributions, but here the coherent dipole mode instability can occur due to the perturbation of phase space distribution. Bunch displacement grows exponentially at first, and then goes into saturation. By using the realistic phase space distributions instead, irregular single particle motion is not associated with a coherent dipole instability.

5 Intensity limits for both RF systems

5.1 Self-consistent phase space distributions

For long bunches, neither the external voltage nor the SC induced voltage will be still linear. Even for large tune spread of single particles, stationary phase space distribution $\psi(p,\phi)$ for a bunch with the maximum of phase extension $\phi_{\rm m}$ is obtained by using:

$$\psi(p,\phi)\sim f(H(\phi_{\rm m})-H(p,\phi))\,, \tag{4}$$

where $H(\phi_{\rm m})$, $H(p,\phi)$ are the Hamiltonian of the particle with phase space coordinates (p,ϕ), and p is the momentum.

The Vlasov equation leads to the time independent phase space distribution $\psi(p,\phi)$:

$$\frac{{\rm d}\psi}{{\rm d}t}=\frac{\partial\psi}{\partial t}+\frac{\partial\psi}{\partial\phi}\frac{{\rm d}\phi}{{\rm d}t}+\frac{\partial\psi}{\partial p}\frac{{\rm d}p}{{\rm d}t}=0\,. \tag{5}$$

In the presence of SC forces, $\psi(p,\phi)$ is greatly simplified by using the Hofmann-Pedersen approach, a local elliptical distribution function[7, 8]:

$$\psi(p,\phi)=C\sqrt{\hat{H}(\phi_{\rm m})-\hat{H}(p,\phi)}\,, \tag{6}$$

where C is given by the kinematical factors.

The resulting line density $\lambda(\phi)$ is given by:

$$\lambda(\phi)=\int\psi(p,\phi){\rm d}p=\mu_\Phi(\Phi(\phi_{\rm m})-\Phi(\phi))\,, \tag{7}$$

where $\Phi(\phi)$ is the RF potential, and μ_Φ normalizes the integrated line density to one. For the dual harmonic RF system, the normalization factor μ_Φ depends on both, the maximal phase extension $\phi_{\rm m}$ and the parameter d. Short bunches in single harmonic system leads to elliptical phase space distribution with parabolic line density. Only for the Hofmann-Pedersen approach, where the line density is determined from the external RF potential, increasing the voltage by factor $R(N)$ keeps the distribution unchanged.

The coherent dipole mode instability occurs, if the dipole mode frequency is outside the synchrotron frequency range[9]. Keeping bunch length unchanged with particle number N requires an increase of the external voltage by factor $R(N)$ to compensate the SC

voltage, keeping effective voltage unchanged. Limiting incoherent tunes are also unchanged: $\omega_{\rm s}^{\rm max}=\omega_{\rm s0}$ for d=0 at small phase values resp. $\omega_{\rm s}^{\rm max}=0.8\omega_{\rm s0}$ for d=0.31 at 2 rad. but the coherent dipole mode frequency $\omega_{\rm D}(N)$ depends on $R(N)$:

$$\omega_{\rm D}^2(N)=\omega_{\rm s0}^2R(N)(f_1(\phi_{\rm m},d)/f_2(\phi_{\rm m},d))^2\,,$$

where

$$\begin{aligned} f_1^2(\phi_{\rm m},d)=&\ \phi_{\rm m}(1+d^2)-2d\sin\phi_{\rm m}-0.5\sin2\phi_{\rm m}+\\ &(2d/3)\sin3\phi_{\rm m}-(d^2/4)\sin4\phi_{\rm m}\,,\\ f_2^2(\phi_{\rm m},d)=&\ 2\sin\phi_{\rm m}-(d/2)\sin2\phi_{\rm m}-\\ &2\phi_{\rm m}\cos\phi_{\rm m}+d\phi_{\rm m}\cos2\phi_{\rm m}\,. \end{aligned} \tag{8}$$

5.2 Intensity limits for long bunches

Dipole mode correction factor $f_1(\phi_{\rm m},d)/f_2(\phi_{\rm m},d)$ is shown in Fig. 6 for d=0 and d=0.31: small phase extension decreases the correction factor by $\sqrt{1-2d}$, but the matched voltages V_0 are different for both cases. For both cases, the dipole mode frequency has similar dependence on the maximum of phase extension $\phi_{\rm m}$ as unperturbed synchrotron frequencies[5]. The r.m.s phase values are dependent on both maximum of phase extension $\phi_{\rm m}$ and parameter d. A r.m.s phase value of 0.78 rad corresponds to the maximal phase extension $\phi_{\rm m}$ of 1.75 rad (d=0) resp. 2 rad (d=0.31).

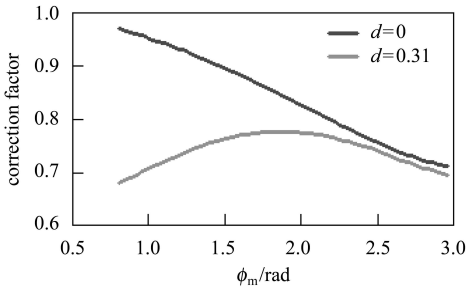

Fig. 6. The frequency correction factor for single and dual harmonic.

For the matched long bunches, rigid dipole mode instability occurs in the single harmonic system for $R(N)>2$, whereas for d=0.31 the intensity threshold is lowered to $R(N)$=1.3 only. The intensity thresholds for the dual harmonic system with d=0.5 are calculated in Ref. [9]. Staying below the threshold intensity, adding resistive impedance components can cause instability. The rise time is dependent on both the resistive impedance and incoherent tune spread[10]. The dipole amplitude goes into saturation, but the phase space distribution is changed.

5.3 Dipole oscillation for realistic input

Using realistic distributions instead of self-consistent ones, the resulting phase space plots after 2×10^4 turns are shown in Figs. 4 & 5 for modest or high intensities in the dual or single harmonic system. The modest intensity of N=10^{13}, $R(N)$=2 is 3 times more than the intensity threshold for the dual harmonic RF system with d=0.31. High intensity of N=4×10^{13}, $R(N)$=4, is also 3 times greater than the intensity threshold for the single harmonic RF system with d=0.

In Fig. 7, the coherent dipole oscillations are shown for the matched elliptical input and resistive impedances of $Z_{//}/n$=50 Ω for n=1,4. Small resistive impedances at low frequencies in addition to large SC impedance of 500 Ω up to high harmonics leads to coherent dipole oscillation around the equilibrium value, approximately given by 50% of the first maximal value.

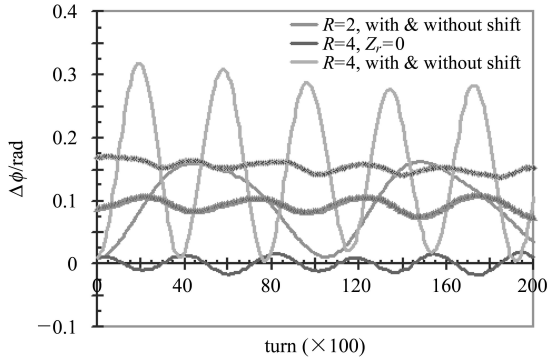

Fig. 7. The coherent dipole oscillation for the emittance & SC-dominated bunches.

The equilibrium phase value is the balance between the energy loss by resistive impedance and the energy gain from the RF system. As the matched RF voltages are enlarged by the factor $R(N)$, the equilibrium phase value does not increase linearly with the particle intensity. The forced energy oscillations are shown in Fig. 2. The behavior is almost unchanged by the resistive impedances.

Without the resistive impedances, shown in Fig. 7 are also the undamped coherent dipole oscillations around the phase axis for high intensity beam where the distribution is changed, see Fig. 5. These coherent oscillations around zero equilibrium phase value are quite similar to the oscillations around zero equilibrium energy value for modest intensity, see Fig. 2, where the distribution is unchanged, see Fig. 4.

Different from the stationary distributions, the tune spreads from the RF and SC voltage, associated with the derivative of line density, are not identical. The initial mismatch will influence the behavior of dipole amplitude, and weaken the effect for curves in Fig. 7. But increasing the resistive impedances will lead to much larger phase offset, and may cause debunching and therefore hinder the coherent dipole oscillations around the equilibrium phase values.

5.4 Coherent dipole instability for short bunches

For short bunches, where the RF acceptance is much larger than the bunch area, the incoherent particle motion cannot lead to debunching, but the coherent dipole mode instability can occur. The initial bunch displacement grows exponentially, and goes into saturation as large displacement stabilizes the dipole instability, associated with the large r.m.s emittance growth[10]. The onsets of instability and growth rate are dependent on the RF waveform. Ignoring the tune spread, the growth rate increases like $n \times \sqrt{Z/n}$.

If the rise time is shorter than the synchrotron oscillation period, the microwave instability occurs. Short bunches and high frequency resistive components can lead to very large coherent growth rates. The onset of microwave instability is described by Keil–Schnell criteria[4, 5], it is independent of the RF amplitude and waveform. Saturation of microwave instability for costing and bunched beams is discussed in Ref. [11].

6 Summary

The mismatch and collective effects can cause debunching for long bunches, if the RF acceptance is too small. The coherent and incoherent effects are analyzed by the new voltage factor $R(N)$, thus simplifying physics. Irregular single particle motion is not associated with the coherent dipole instability.

For stationary phase space distribution of the Hofmann-Pedersen approach and for single or dual harmonic RF system with d=0.31, the stability limits are proved too low if using realistic input distributions. Small resistive impedances lead to coherent oscillations around the equilibrium phase value even for high intensity, as energy loss by resistive impedance is compensated by the energy gain of the RF system.

For high intensity, distribution is changing but the enlarged full RF acceptance hinders debunching. In the dual harmonic system with its enlarged RF voltage for great phase value, much less particles are suffering from debunching.

All results are valid for staying below transition.

Gratefully acknowledged are many useful hints from J.A.Holmes and S.Cousineau, SNS Oak Ridge, USA, about how to use ORBIT code. Shizhong An would like to thank FZ-Juelich, Germany, about financing his stay in Germany and IKP colleagues for all their helps and lots of useful discussions.

References

1 AN S Z et al. Chinese Physics C, 2008, **32**(1): 60
2 Holmes J A et al. ORBIT User Manual, SNS-ORNL-AP TN0011. 1999
3 FAIR Facility, Base Line Technical Report. July 2006, Volume 2, HESR Section 2.11. http://www-new.gsi.de/documents/DOC-2006-Jul-40-1.pdf
4 Chao A W. Physics of Collective Beam Instabilities in High Energy Accelerators. New York: John Wiley&Sons, 1993
5 Ng K Y. Physics of Intensity Dependent Beam Instabilities. Singapore-New Jersey-London- HongKong: World Scientific Publishing, 2006
6 Boine-Frankenheim O et al. PAC Portland, 2003. 2607
7 Neuffer D. IEEE Trans. Nucl. Sci., 1979, **NS-26**(3): 3031
8 Hofmann A, Pedersen F. IEEE Trans. Nucl. Sci., 1979, **26**: 3526
9 Boine-Frankenheim O et al. Phys. Rev., ST Accelerators and Beams, 2005, **8**: 034201
10 LIU Y. HEP & NP, 2003, **27**(12): 1128 (in Chinese); GSI-ACC-Report-2004-02-001
11 Boine-Frankenheim O, Hofmann I. NIM, 2001, **A464**: 351